From Disruption to Destruction Assessing the Impact of High-Power Microwaves on Unmanned Aerial Vehicles

Kacper Karcz[1,2], Andrzej Sitkiewicz[1,2], Janusz Błaszczyk[1], Zygmunt Mierczyk[2]

Air Force Institute of Technology, Warsaw, POLAND

[2] Military University of Technology, Warsaw, POLAND

kacper.karcz@itwl.pl

ABSTRACT

Unmanned Aerial Vehicles (UAVs) have become increasingly affordable and popular, finding applications in various fields, including military reconnaissance and threat of using them as projectiles. These small and agile UAVs pose a challenge for traditional interception methods due to their high speeds, maneuverability, and ability to evade detection. Effective countermeasures are necessary to mitigate the risks associated with UAV. In this paper conclusions from research in the topic of protection and defense of aerial vehicles from high power microwave impulses are presented. An investigation of high-power microwaves (HPMs) impact on AVs was conducted. HPM generator based on an impulse compressor was used in research. Compression allowed for producing impulses with fields intensity exceeding 50 kV/m and power ~3 MW. Employed measurement stands included an HPM generator in both land and sea setups on traverse, as well as reverberating chambers in laboratory. ANSYS simulation software was utilized for planning and assessing the measurement stands, as well as validating the experimental measurements. High-power d-dot and b-dot microwave probes were utilized, along with field intensity loggers, to measure and analyze generated filed distributions. Conducted tests included analyzing the response of UAV when subjected to intense HPM radiation. The tests provided examples of soft and hard-kill of UAVs caused by HPM impulses. Experimental findings show thresholds in filed magnitude above 50V/m were found to induce soft-kill effects, known as lock-up meant as permanently disruption of UAV systems. Furthermore, at intensities above 50kV/m, burnout effects were repeatable, primarily attributed to the thermal destruction of electronic components. The researchers also point out instances of structural damage in UAV mechanical components, directly caused by radiation. Discussed examples of failing of faraday shield caused by structural flexing show that directed microwave weapon is appropriate unwanted UAVs countermeasure. The results of this study highlight the efficacy of HPM pulses as a viable solution for protecting against unwanted UAVs. By leveraging the technology of precise control and manipulation of electromagnetic radiation, it is possible to incapacitate UAVs through both electronic and structural vulnerabilities. The implementation of an appropriate beam control system, and the potential to scale the radiation intensity by adjusting the generator system is an issue that has to be addressed for HPM weapons to be reliable shield against UAVs.

INTRODUCTION

In recent years, we have witnessed a surge in the commercial availability and deployment of unmanned aerial vehicles (UAVs), a phenomenon fueled by the agility and speed of these devices which can readily reach speeds up to 150 km/h. This meteoric rise poses new security and defense challenges on a global scale as current Russo-Ukrainian war demonstrates. The construction materials of UAVs — including plastic, epoxy, and fiberglass — yield a low radar cross-section, necessitating the adoption of optoelectronic techniques for effective detection. Particularly in the case of racer UAVs, which are capable of achieving speeds of up to 200 km/h, there is a pressing requirement for rapid response measures, with a reaction window as narrow as 1-2 minutes post-detection considering their low-altitude flight and horizon distance. Moreover, adept operators utilizing first-person view (FPV) goggles can deftly maneuver swift UAVs, presenting a substantial challenge to physical interception strategies, which become almost untenable.

Motivated by this complex landscape, our research sought to explore the potential of compact High-Power Microwave (HPM) sources in remotely interacting with aerial vehicles to induce disruption, lock-up, or even burnout of their digital systems. In the army, the nomenclature of soft-kill and hard-kill is used. In the case of a UAV, any permanent disruption to the operation of one of the key systems ultimately results in its kill. The team therefore adopted a nomenclature in which soft-kill is defined as a state in which the system does not return to proper operation after the radiation has ceased. This endeavor is grounded on the critical vulnerabilities intrinsic to UAVs: their heavy reliance on semiconductors and MEMS systems, which, while essential for orientation through acceleration and barometric measurement, are highly susceptible to induced electromagnetic (EM) disturbances. Recognizing that digital transistor systems are vulnerable to impulse damage, we investigated strategies to exploit these and other weaknesses to inhibit the principal functionalities of UAVs.

Building upon preliminary studies conducted at the Laboratory of Electromagnetic Compatibility and Electromagnetic Field Measurements, a part of the Military Institute of Armament Technology in Zielonka, our approach employed radiation signals with frequency ranges between 200 MHz and 18 GHz and intensity levels spanning 10, 20, and 50 V/m to examine the most effective field attributes in neutralizing aerial vehicles. A detailed account of this phase of the research is available in our earlier publication [1].

Our current investigation forms a segment of the broader research project entitled “Methods and Means of Protection and Defense against HPM Impulses,” an initiative under the strategic program for state defense and security, focusing on “new weapons and defense systems in the field of directed energy.” This project revolves around the exploration of shielding strategies and mitigation approaches against HPM irradiation. We delved into the impact of HPM impulses on a plethora of digital systems found in commercially available UAVs and other consumer electronics such as phones, smartwatches, and basic electronic circuits embodying flashing circuits or autopilot systems. Our research leveraged a 3 MW system to achieve field intensities exceeding 50 kV/m, utilizing the facilities of the reverberation chamber housed at the Naval Academy in Gdynia, and field tests conducted on land and marine platforms with a parabolic antenna.

Based on the findings of our research, we hypothesize that compact HPM generators with the current state of technology may be able to remotely neutralize at least one of the critical digital systems of aerial vehicles from a sufficient distance. We have outlined the ranges of field intensity at which each of these effects — disruption, lock-up, and destruction — can be attained. We claim to have identified the threshold field intensities that guarantee the disruption, freezing, or destruction of an unprotected aerial electronic system. The compact high-power microwave (HPM) pulse source, when equipped with a suitable beam or beam steering system, has the potential to function as the primary component of the air denial system for unmanned aerial vehicles (UAVs).

Furthermore, our research outcomes provide insights into the consequences of High-Power Microwave (HPM) impulses on the mechanical integrity of Unmanned Aerial Vehicles (UAVs). In addition, we examine the effects resulting from exposure to power levels that are sufficiently high to surpass the reflecting electromagnetic shielding provided by Faraday cages.

2.0 MATERIALS AND METHODS

2.1 Experimental Procedures

2.1.1 Research Station at AMW

The qualitative aspect of the research predominantly unfolded at the High-Power Microwave (HPM) research station situated at the Naval Academy in Gdynia. Central to this facility is a metal container that houses the pulse generator, cooling system, and an internal reverberating chamber. Connection with the

generator was established via a WR284 waveguide filled with sulphur hexafluoride (SF6) gas, maintained at a pressure of 800 hPa. The impulse was radiated thru a LB-284-20 horn antenna, installed within the electromagnetically shielded WAVECUBE reverberation chamber.

Figure 1: Reverberation chamber and generator setup.

This chamber does not have any absorbent layers, so it only serves the function of isolating electromagnet its inner space. This results in multiple reflections and superimposition of the radiation pulses, thereby causing local amplification and attenuation of the radiation intensity.

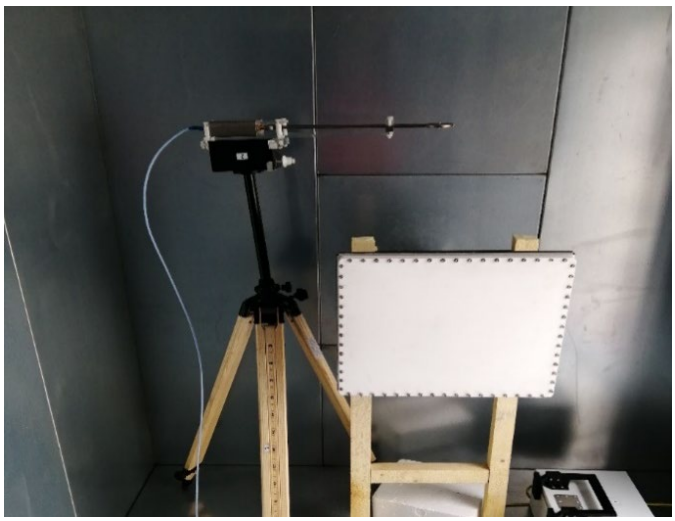

Figure 2: Field intensity measurement system.

Measured shape of the envelope of the impulses recorded in the chamber suggests that their frequency changed during the generation of some of them.

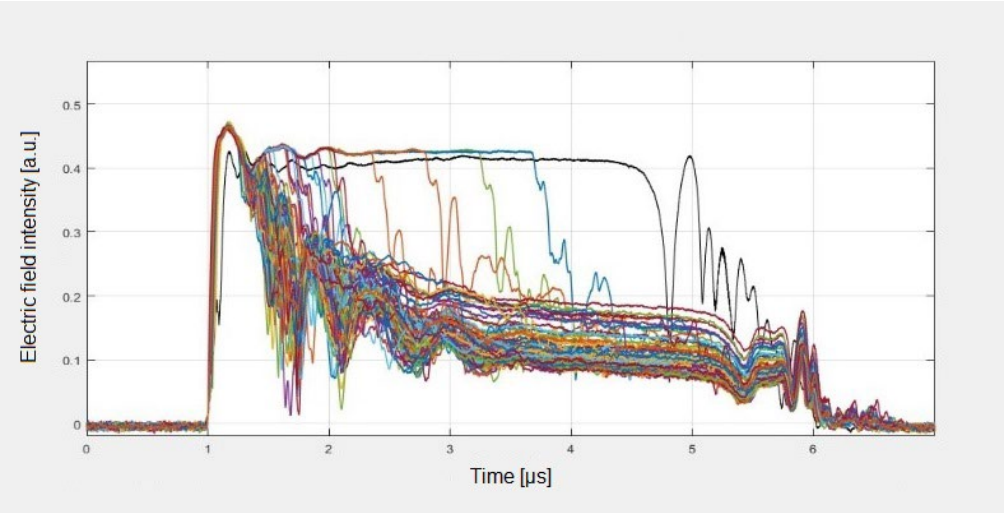

Figure 3: Superimposed series of envelopes of generated pulses of varying duration and shape.

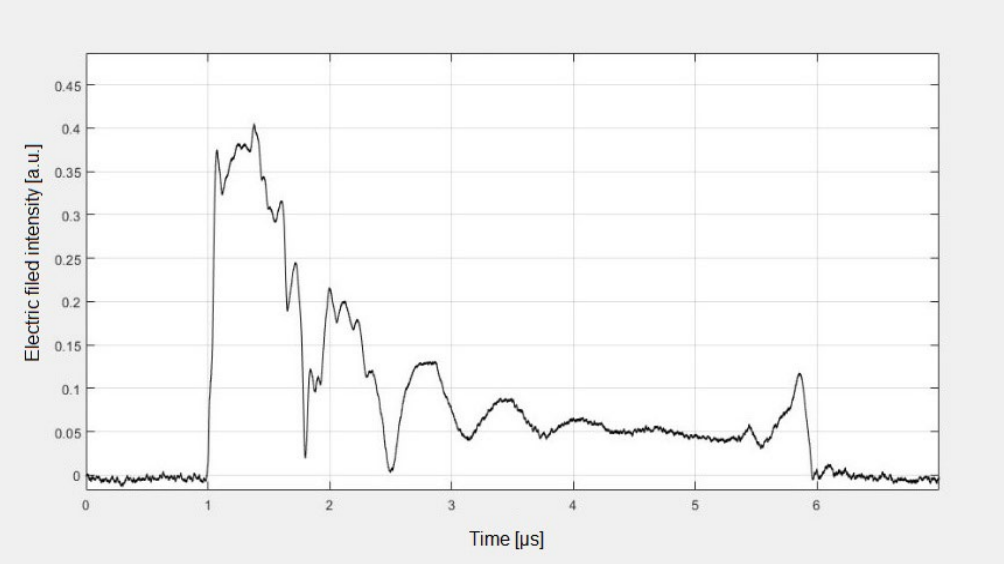

Figure 4: Signal envelope ripples (bursts of the directly incident wave and reflected waves with changing phases).

The phenomenon described can be observed as a ripple effect, characterized by the fluctuation of signal amplitude resulting from the combination of the direct signal and multiple reflected signals with varying frequencies and corresponding phase differences, leading to a field distribution that can be reproduced consistently. The observed outcomes are likely associated with the characteristics of electromagnetic wave reflections within the chamber. To clearly determine the exact measurement locations, a three-dimensional coordinate system (x, y, z) was adopted, which begins in the lower left corner of the chamber, opposite the antenna wall.

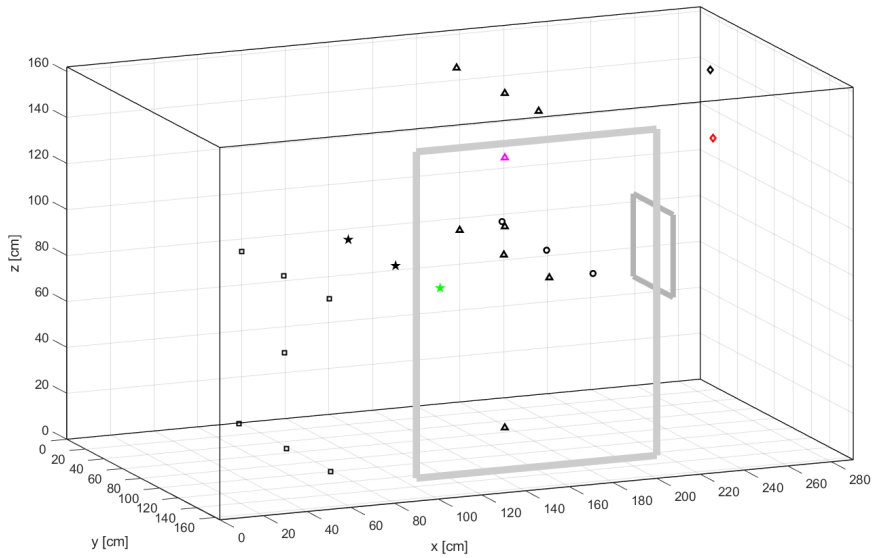

Figure 5: General model of the chamber with the points where measurements were taken (the outline of the door and antenna marked).

During the experimental procedure, the hi-power montena SFE3-5G probe, shielded BL3-5G montena balun, and MOL3000 optical transmitter were positioned within the container of the tested chamber, where the transmitting antenna was situated. The remaining portion of the measurement track was situated in a separate container, which also housed the generator control system.

Measurement Points and Results:

- Maximum value: Documented at coordinates (x, y, z) = (261, 82, 125) with a peak intensity of 54 kV/m.
- Minimum value: Documented at coordinates (x, y, z) = (114, 134, 84) with a peak intensity of 8.4 kV/m.

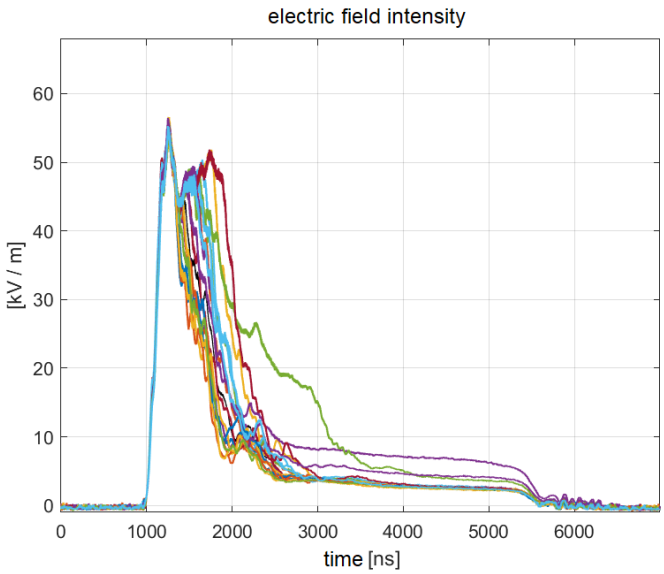

Figure 6: The electric field intensity for spatial coordinates: X= 261cm, Y=82cm, Z=125cm.

2.1.2 Land and Sea Research Stations at the Ustka and Nowa Dęba traverse

A study was conducted to examine the quantitative effects of the HPM pulse on commercially available UAVs. This research was conducted at a shooting range as part of the product testing for the project focused on protecting aviation equipment against directed energy weapons. The objective was to validate the attainment of the technology readiness level by the utilization of the designed air-tank container that embodies the technology. As part of the conducted research, UAVs were successfully rendered inoperable inside a marine setting, specifically on a level expanse of sandy terrain devoid of significant territorial impediments. Additionally, the UAVs were subjected to destruction within a clearing encompassed by a mixed forest comprising both deciduous and coniferous trees.

2.1.3 Sea-Based Research Station

For the maritime segment of the experiment, four buoyant units were employed: one equipped with generators accompanied by cooling and power systems, and the other harboring control and measurement apparatus, alongside a raft for situating the subject of the research and small operational motorboat.

Figure 7: Parabolic antenna used in research.

The specifications of the utilized generator and antenna systems were as follows:

Generator Specifications:

- Manufacturer: NCBJ
- Transmitter type: Microwave impulse generator grounded on a magnetron
- Generated frequency: 2.98 GHz
- Pulse power: 3 MW
- Pulse duration: 0.5 – 3 μs
- Pulse repetition period: Ranging from a single pulse to 4 ms
- Rising front slope time: 0.1-0.2 μs
- Falling rear slope time: 0.2-0.5 μs
- Integration: Direct waveguide incorporation with a directive antenna

Parabolic Antenna Technical Data:

- Frequency working range: 2 – 3.5 GHz
- Main lobe directional gain: 32 dBi
- First side lobe directional gain: Approximately 20 dBi
- Horizontal plane beam width: 5 ± 0.7°
- Vertical plane beam width: 3.5 ± 0.7°

Connections to the generators were orchestrated through a WR284 waveguide filled with SF-6 gas at a pressure of 800 hPa. This maritime research phase utilized a raft for hosting the research subject designed for exposure, secured to a grounded copper plane measuring 5 x 3.75 meters. The tests involved exposing shielded air-tank container, embodying electronics such as autopilot systems, video cameras, and elementary circuit boards with blinking diodes, to the HPM impulses both in and in container and in its proximity. Racer type UAVs, while hovering above the raft, were similarly subjected to HPM impulses. The expected distance between the antenna and the drones is around 100 meters, resulting in an estimated intensity of 3.7 kV/m.

2.1.4 Land-Based Research Station on traverse in Ustka and in Nowa Dęba

The land-based portion of the study leveraged the identical generator setup endowed with power and cooling units, coupled with the same parabolic antenna through a WR284 waveguide filled with SF6 gas sustained at a pressure of 800 hPa. Antenna land footing was integrated into setup, allowing movement in azimuth axis.

Figure 8: HPM impulse generation setups.

To ascertain field intensity and maintain consistency across the test location, D-dot field probes, shielded impedance transformer fiber optic links, and a PC data acquisition system were utilized. The vertical polarization of the antenna signal's E-vector was defined. Field intensity of the electric field was appraised using a measuring system based on montena D-dot probe.

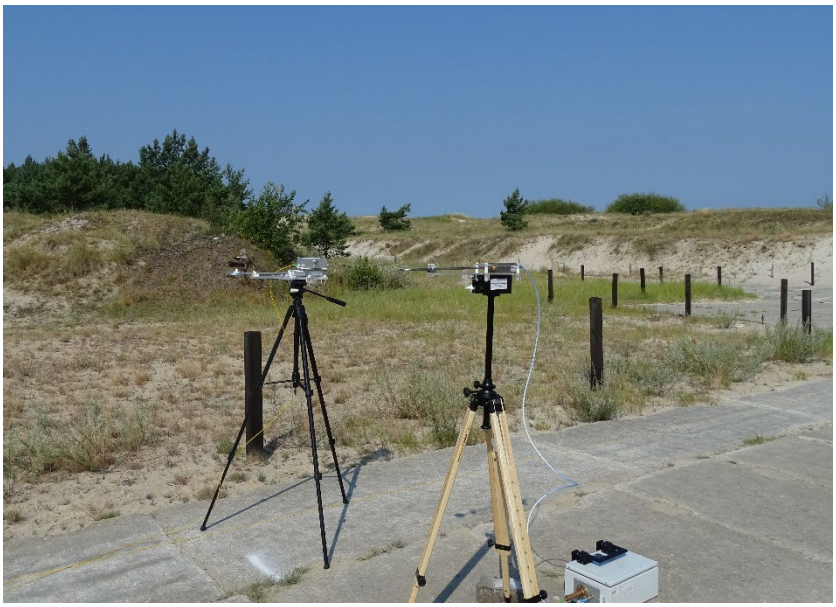

Figure 9: Measured electric field intensity distribution; particular measurement amounted 17.0 kV/m at a distance 23 m.

3.0 RESULTS

3.1 Land-Based Research at HPM Research Station at the Naval Academy in Gdynia

In the reverberation chamber of the Naval Academy in Gdynia, experiments were conducted to scrutinize the impact of pulses on various electronic systems. Different devices including telephones, smartphones, smartwatches, and UAVs were placed at various points in the chamber characterized by varying radiation intensities to study the effects. It was observed that devices consistently exhibited no malfunctions when placed in areas with similar radiation levels and repeatable damage were obtain in certain chamber spots at higher intensities did so invariably. The UAV Syma X8PRO demonstrated significant vulnerabilities to high radiation intensities, enduring severe damages including circuit burns and motor malfunctions.

Subsequently, experiments were conducted to capture a visual recording of the candle flame while it was subjected to exposure within the chamber. Mobile phones that were placed in the chamber were utilized for this purpose:

1) Sony Ericson Xperia Neo V - 2 pcs.
2) Sony Xpreria L -2 pcs
3) Huawei P8 Lite - 1 pc
4) Balupunkt FL-01 -6 pcs

With exposure conditions:

- Pulse power: 2 MW,
- Pulse repetition frequency: 5 Hz,
- Number of pulses: 25.

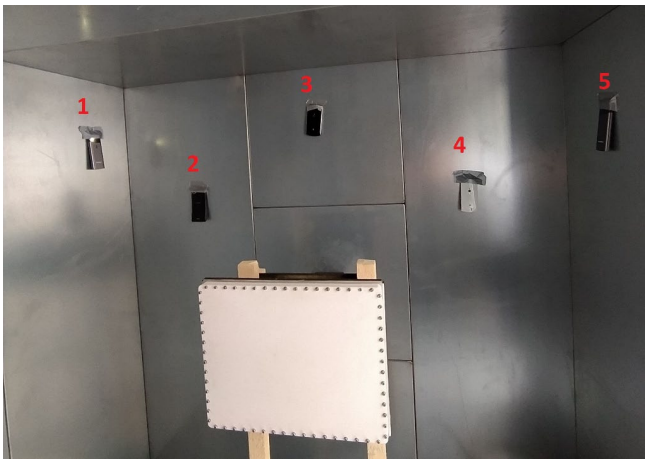

Figure 10: Placement of phones in the chamber.

After performing the exposure in the configuration shown in the figure and verifying the condition of the mobile phones, it was found:

1) (Balupunkt FL-01) Works, but gets very hot. The battery level dropped from almost full to empty within 2-3 minutes.
2) (Huawei P8 Lite) It turned off. After restarting, no damage was found. The phone connects to the network and allows you to make a voice call.
3) (Sony Ericson Xperia Neo V) Turned off. After restarting, no damage was found. The phone connects to the network and allows you to make a voice call. It was found that the recording turned on before the test and saved on the SD card was damaged.
4) (Sony Xpreria L) It turned off. After restarting, no damage was found. The phone connects to the network and allows you to make a voice call. The camera has been damaged (a system error appears after trying to open the camera application).
5) (Balupunkt FL-01) Turned off. After restarting, no damage was found. The phone connects to the network and allows you to make a voice call.

Therefore soft-kill was obtained for all of the DUTs. These experiment were conducted persistently. Further, it was examined how the operation of individual subsystems or functionalities affects the impact of the pulse on the DUT. It was noticed that the operation of the component significantly increases the probability of its damage. For example when phones were set to record a video, camera would break after irradiation, when video is set to play display gets damage.

Figure 11: Damage to the phone's display.

UAVs were also exposed to exposure in a series of destructive tests. It was placed in the switched-on chamber at the coordinates x = 114 cm, y = 86 cm, z = 83 cm (the measured intensity at the point is $\overline{E}_{\max}$ = 34 kV/m, $\sigma_{E_{\max}}$ = 0.3 kV/m) and then subjected to exposure.

Exposure conditions:

- Pulse power: above 2 MW,
- Pulse repetition frequency: 5 Hz,
- Number of pulses: 25.

After opening the chamber, it was discovered that all four of the UAV's engines had ceased functioning. The issue was resolved by performing a reset by the removal and reinsertion of the battery. The UAV then underwent a second exposure. In this instance, the parameters of the generator were set for an infinite quantity of pulses, and it was activated for a duration of thirty seconds. Following the reopening of the chamber, the odor of smoldering plastic could be detected. The UAV exhibited a lack of responsiveness to external stimuli, with only two out of the four engines in operation. Upon the removal and subsequent reinsertion of the battery, the aforementioned motors exhibited immediate spinning upon the application of power, without any activation of the UAV.

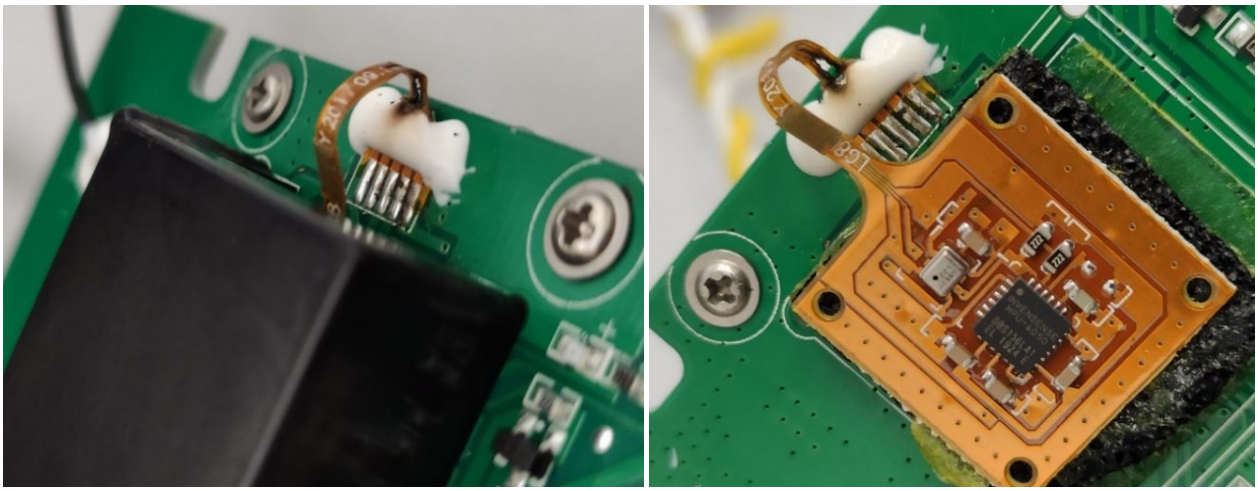

Figure 12: Damage to the wiring harness.

A burnt position light board was also found. Apart from the fact that all the electronic components present on the LED light board were burned, the plastic of the housing in its immediate vicinity was also damaged.

The plastic gears responsible for the camera's angle setting were also damaged. After closer examination, plastic burning was found in the immediate vicinity of the electric motor, but in a place where there are no electrical connections or electronic components. The plastic attaching the end of the steel rod acting as a mechanical support was burned.

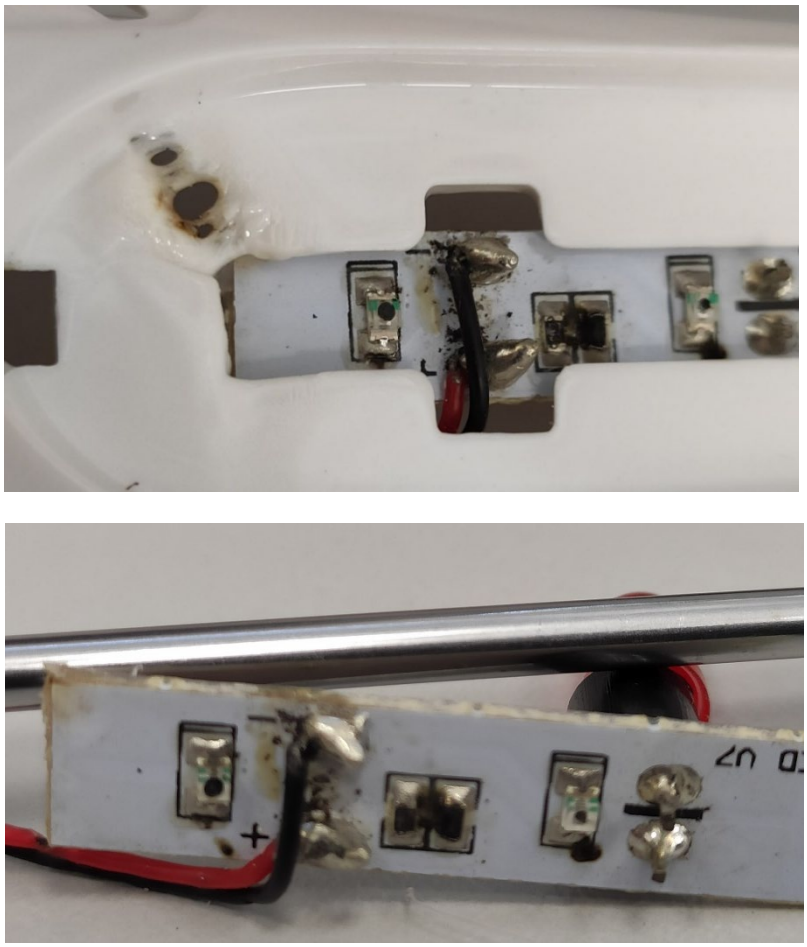

Figure 13: Position light board.

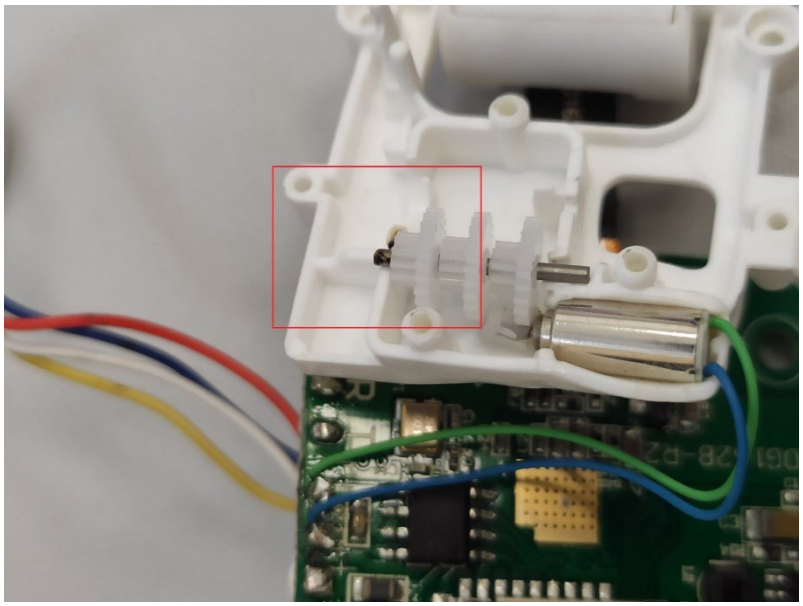

Figure 14: Damage to gears.

Following the completion of the testing, the Unmanned Aerial Vehicle (UAV) underwent a disassembly process in order to visually inspect its components for any observable signs of damage. The examination revealed the presence of damage to the strip cable harness that directly connects to the central unit. Upon microscopic examination, the control system exhibits no observable indications of physical harm.During the experimental trials, a camera placed within a shielded air-tank container recorded the surroundings using a shielded optical track. Since the WAVECUBE chamber lacked an internal light source when closed, tea-light candles were placed near the antenna to provide illumination. During the period of HPM exposure, the phenomenon of flashing or plasma generation was observed.

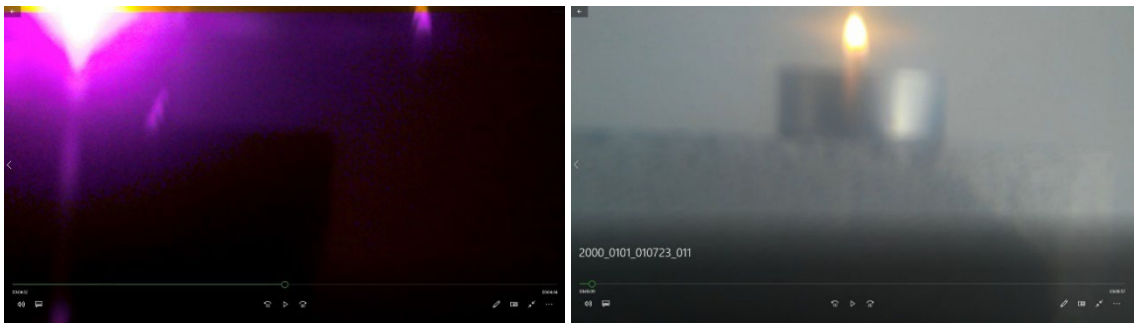

Figure 15: Stills from the video by camera in DUT.

3.2 Sea-Based Research in Ustka

3.2.1 On-Raft Measurement

The electronic systems on the raft experienced various levels of disturbances. The video recordings inside the shielded compartment of the container remained uninterrupted, while the external camera experienced a lock-up, resuming normal function after a battery reset but resulting in a damaged video file. Autopilots placed at different heights above the grounded surface of the raft documented the effects vividly, exhibiting strong spikes potentially due to HPM impulse because accelerations of the order of 1.5G while drifting in calm seas are unlikely, a clear indication of the strong field presence during at least three of the five shots taken.

3.2.2 In-Flight Measurement

- Control Flight

During this segment, the UAV maintained optimal response rates to operator commands, indicating a successful control flight devoid of electromagnetic interference.

- Flight 1

The UAV exhibited resilience to the pulse with parameters f_{rep} = 50 Hz, P = 1.5 MW, maintaining control and functionality before and after pulse generation. Possible explanation is a miss of the radiation beam or inadequate couplingto UAV systems.

- Flight 2

This flight demonstrated the dire consequences of high-frequency electromagnetic interference. HPM impulse with parameters f_{rep} = 150 Hz, P = 1.5 MW, caused total loss of control and resulting in a crash. The parameters highlighted the significant increase in pulse frequency, revealing the vulnerable threshold of the UAV system.

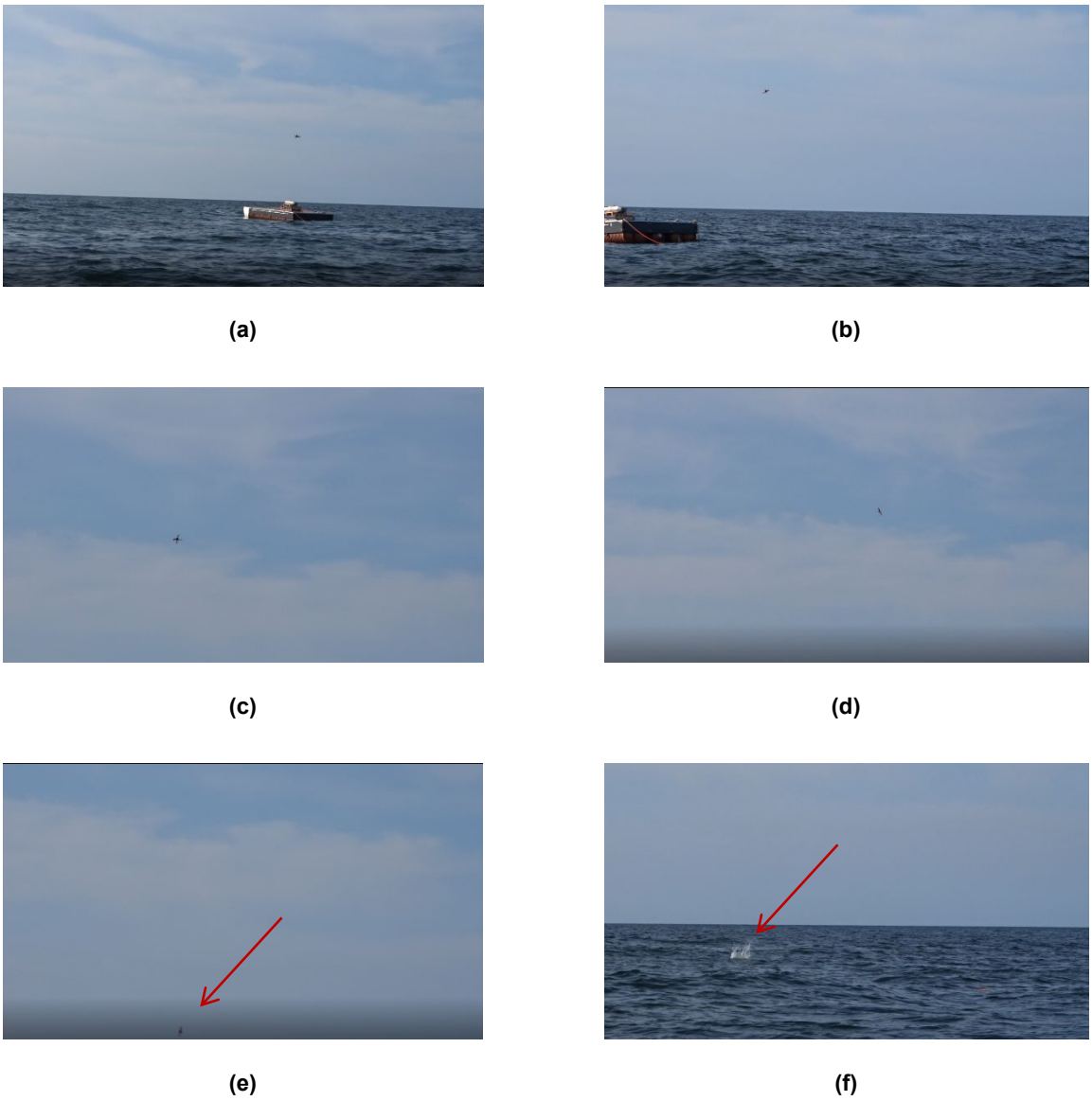

Figure 16: Stages of research flight during exposure a), b) – before exposure; c), d), e), f) – after exposure.

3.3 Land-Based Research in Ustka

3.3.1 Research on Effectiveness of HPM Impulses on UAV Neutralization

During tests conducted over the shooting range, the research achieved consistent UAV neutralization. Despite challenges in determining the exact cause of damages, whether due to direct radiation impact or subsequent fall, the presence of burnout effects was noted in three UAVs. The field intensity estimation affirmed the existence of substantial radiation levels across the range which wouldn't be lower than 3 kV/m, verifying the effective neutralization of the UAVs through HPM impulses.

Figure 17: Stills form video documentation of HPM effect tests.

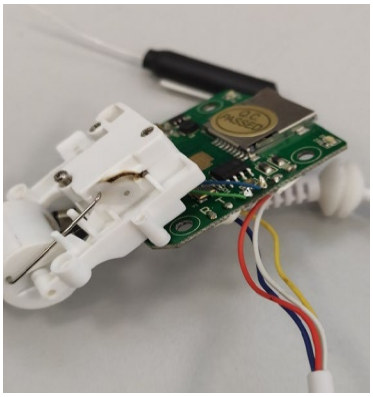

Figure 18: Damage caused by HPM impulse.

3.3.2 Effects of Intensive EM Impulse Observed

Within the ambit of the study, it was noted that the shielded container which, was a main DUT, unexpectedly lost its shielding capability, a phenomenon attributed to improperly aligned shielding structures at the entrance of the microwave radiation dampening vision path. Simultaneously, the ANSYS simulation software played a pivotal role in understanding the electromagnetic dynamics during the leakage. An adaptation of the model incorporating the identified fault allowed a deep dive into the complex modal and resonant behaviors in the shielded enclosure, matching the observed phenomena and highlighting the overriding influence of standing waves within the cavity over the incident wave.

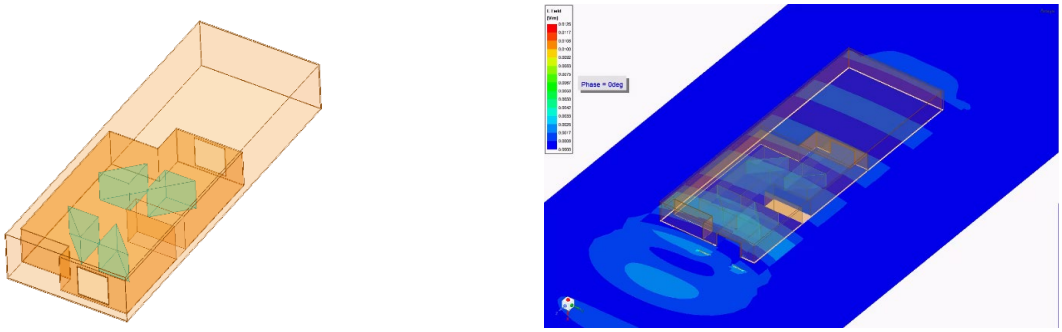

a) b)

Figure 19: Anty-HPM air-tank container model a), with given plane wave beam b).

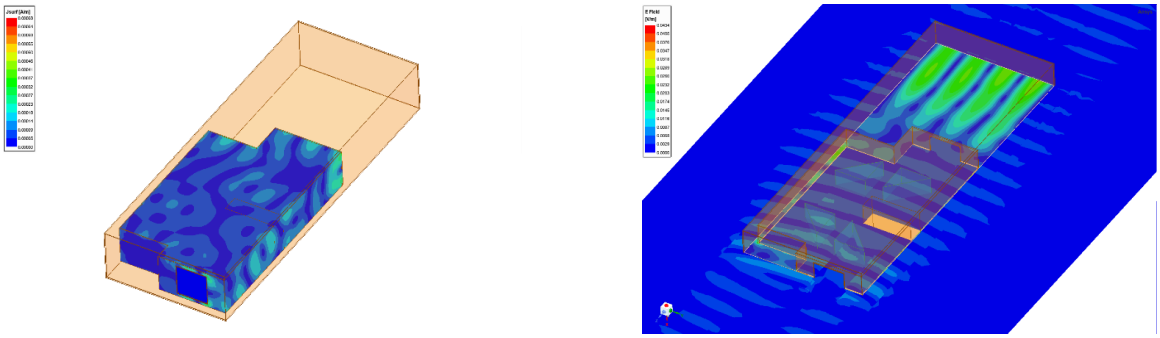

a) b)

Figure 20: Results of the numerical computation a)surface current on inner reflective layer, b) electric field intensity inside container.

3.4 Exposure of UAV Syma X8PRO in Nowa Dęba

A couple of UAV Syma X8PROs were subjected to HPM irradiation were meter registering intensities of 11.2kV with a standard deviation of 0.3kV/m, with detailed pre and post-exposure assessments indicating varying degrees of functional degradation. After each shoot UAVs fell to the ground upon exposure. Setup was made specifically so DUT wouldn't fall from high altitude.

Figure 21: The moment of disabling the Syma UAV by the HPM impulse.

Table 1: State matrix of UAVs during HPM exposures test.

Device	Pre-Exposure Status	Post-Exposure Status #1	Post-Exposure Status #2
UAVX8PRO #1	Fully functional	Soft-kill	Hard-kill
UAVX8PRO #2	Fully functional	Fully functional	Soft-kill

3.4.1 Analysis of the Damaged UAV Syma X8PRO #2

A meticulous analysis of the permanently damaged UAV Syma X8PRO #2 revealed that aside from minor temperature-induced alterations at one of the transistor legs, no other substantial visible damages were found. The transistor was associated with motor rotation control. Further, it was found that the MOSFET transistors controlling the brush motors operation had been damaged despite their Schottky diode protections. Post-connection to the battery, voltage was present in all four electric motors, but only one was operational. Dismantling the uncontrollably spinning motor revealed seriously burned coils, indicative of potential short circuits between the windings.

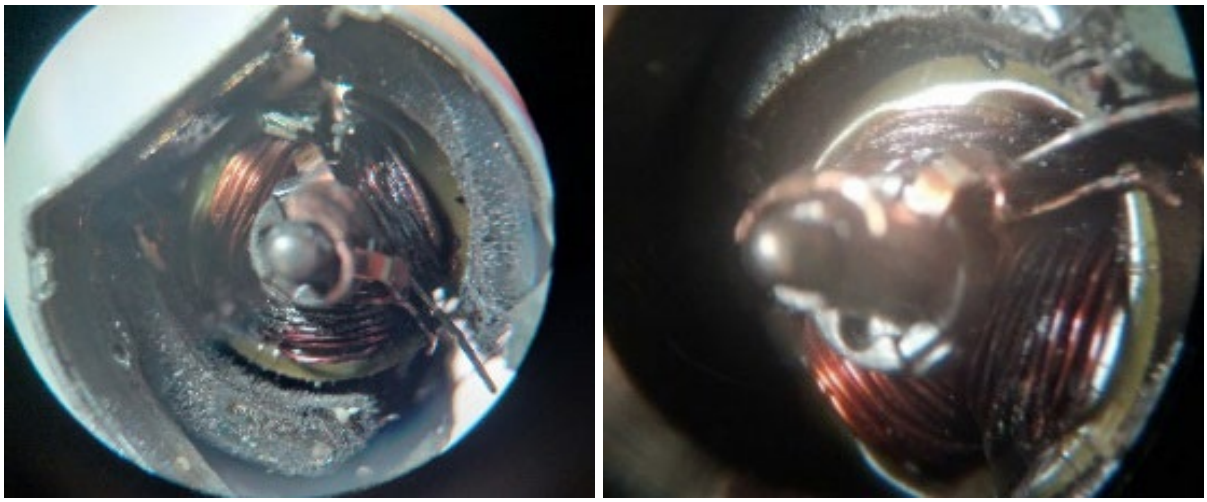

Figure 22: Microscopic photo of burnt electric motor windings.

4.0 DISCUSSION

The vulnerabilities of UAVs to HPM impulses were clearly demonstrated across the range of tests conducted, revealing significant susceptibilities to induced electromagnetic (EM) disturbances given their heavy reliance on semiconductor and MEMS systems. The Syma X8PRO UAVs, in particular, displayed substantial vulnerabilities, with numerous instances of disruptions, suspensions, and even destruction occurring with confidence at field intensities exceeding 50 kV/m. The findings highlight the pivotal role of impulse parameters, such as frequency and power, in influencing UAV resilience to HPM exposures. It was noted that UAVs could withstand certain impulse parameters while succumbing to similar in other circumstances. This establishes a clear mandate for future research to delineate these thresholds meticulously to inform the development of HPM systems capable of neutralizing UAV threats efficiently.

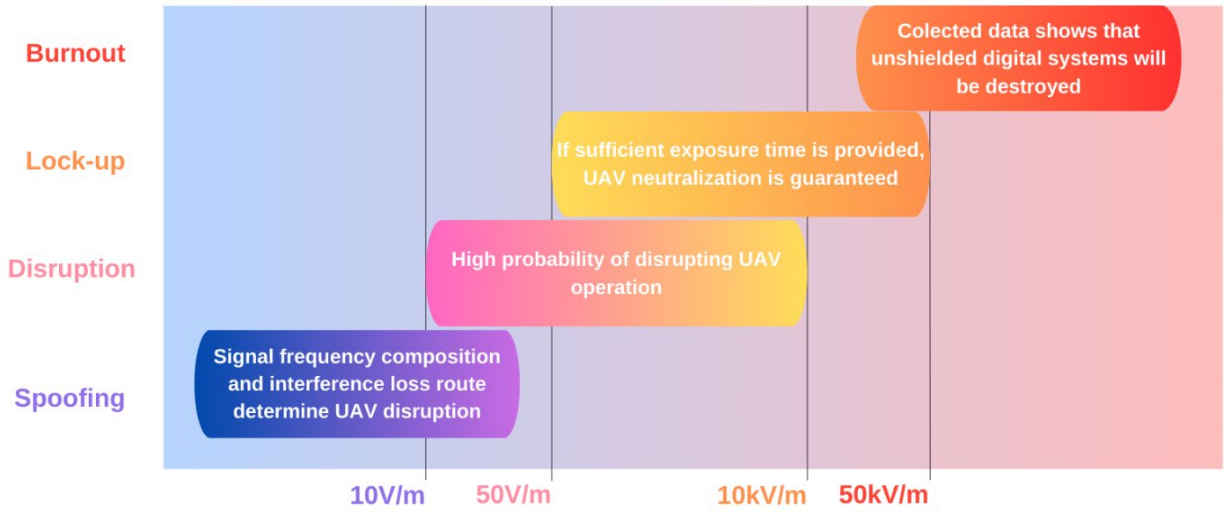

Figure 23: Diagram showing the effects of the impact.

A significant revelation from the research was the potential for the electronics housed in shielded enclosures to withstand HPM impulses, albeit not universally. The findings underscore the necessity for robust shielding solutions to secure UAVs and other critical infrastructural elements against HPM threats.

This study unequivocally illustrates that HPM technologies harbour a significant potential in the realm of defence technologies, especially in countering UAV threats. The effective neutralization of UAVs observed during the tests over the shooting ranges establishes a robust case for the deployment of HPM technologies in critical defence infrastructures. Moreover, the exploration of the impact of HPM impulses on a wide array of consumer electronics, including phones and smartwatches, hints at the broader implications of this research.

This research marks a significant stride in understanding the interactions between HPM impulses and UAVs, laying a solid foundation for the future development of HPM-based aerial denial systems. While the study has successfully highlighted the potential of compact HPM generators in neutralizing UAVs remotely, it also underscores the urgency for developing beam guidance system solutions combined with detection and recognition systems.

5.0 LITERATURE

[1] Sulkowski, Jarosław, Błaszczyk, Janusz, Grzybowski, Adam, Karcz, Kacper and Kowaleczko, Paweł. “Investigations of the susceptibility of unmanned aerial vehicles on intensive microwave radiation” Journal of KONBiN, vol.48, no.1, 2018, pp.107-118. https://doi.org/10.2478/jok-2018-0049

[2] M. G. Backstrom and K. G. Lovstrand, “Susceptibility of electronic systems to high-power microwaves: summary of test experience,” in IEEE Transactions on Electromagnetic Compatibility, vol. 46, no. 3, pp. 396-403, Aug. 2004, doi: 10.1109/TEMC.2004.831814.

[3] J. A. S. E. S. James Benford, High Power Microwaves, Second Edition, CRC Press, 2007.

[4] V. S. P. Vladimir Vasilevich Shurenkov, “Electromagnetic Pulse Effects and Damage Mechanism on the Semiconductor Electronics,” Facta Universitatis Series: Electronics and Energetics, tom 29, nr 4, p. 621 – 629, 2016.

[5] M. B. Deveci, Directed Energy Weapons: Invisible and Invincible, Monterey: Naval Postgraduate School, 2007.

[6] L. X. 1. B. Z. 1. H. M. Dong Chen 1, Research on the Effect of High Power Microwave on Low Noise Amplifier and Limiter Based on the Injection Method, Electromagnetic Analysis & Applications vol. 2, 2010.